MODIFIED FAST FOURIER TRANSFORMATION COMPUTATION OF STEERING VECTORS IN VIRTUAL ROTATING ARRAY BEAMFORMING

Ce Zhang[1], Wei Ma[1], Ennes Sarradj[2], Simon Jekosch[2], Gert Herold[2]
[1]School of Aeronautics and Astronautics, Shanghai Jiao Tong University
Dongchuan Road 800, 200240, Shanghai, P.R. China
[2]TU Berlin, FG Technische Akustik
Einsteinufer 25, 10587, Berlin, Germany

Abstract

Virtual rotating array (VRA) beamforming is widely used for rotating sources localization. Steering vectors in the VRA beamforming should take into account the rotation of sound-bearing medium, which causes complexity and low computational efficiency. Computing this type of steering vectors in a simple and efficient way at multiple considered frequencies is a persistent pursuit. A new approach is proposed in this paper to calculate this type of steering vector. In this approach, the sound travel time is obtained via the phase of a summation of modal transfer functions, where each modal transfer function is computed through fast Fourier transformation on the steering vectors of conventional frequency-domain beamforming. Then steering vectors in VRA beamforming at each considered frequency are calculated through the sound travel time. This approach is demonstrated by comparing to time-domain methods method in a benchmark simulation case and an axial fan experiment. The computational efficiency of the new approach is one order of magnitude higher than those of time-domain methods.

1 INTRODUCTION

Rotating sound sources localization have been the research interest in many engineering applications, including wind turbines, axial fans and other rotating machinery [1]. Phased microphone array beamforming has become a useful tool and several beamforming methods have been proposed to analyze rotating sound sources [3, 6, 8, 16]. Among these methods, virtual rotating array (VRA) beamforming [3] has the advantage that deconvolution and inverse methods can easily be used together with it [15].

Steering vector computation, which plays a crucial role in the VRA beamforming, should take into account the rotation of sound-bearing medium to avoid localization deviation [5]. To calculate this type of steering vector, a modal expansion method [7, 12] is proposed based on the exact frequency-domain solution of sound field radiated from a rotating monopole source [11], in which each modal transfer function contains a spherical harmonic series expansion. This method is called the spherical harmonic series expansion method (SHSEM) [7]. SHSEM is computationally inefficient, due to the low computational efficiency of spherical harmonic series calculation [5]. In addition, the steering vector has to be calculated independently for each considered frequency [9]. Researchers then dedicated to improve the computational efficiency of VRA steering vectors.

Time-domain methods were proposed consequently, such as SV-C2 method [5, 12], acoustic ray method [9] and ray casting method [15]. These methods calculate the steering vector through computation of the sound travel time between a rotating source and a virtual rotating microphone. Compared with SHSEM, computational efficiencies of these time-domain methods improve by an order of magnitude for a single frequency, and improve by greater magnitude for multiple frequencies. However, the computational efficiencies of these time-domain methods are limited as they are based on iterative solution of sound travel equations or solving differetial equation systems.

Recently, Zhang & Ma [17] proposed a fast Fourier transformation (FFT) computation method of modal transfer function generated by rotating sources, where the spherical harmonic series calculation in SHSEM is replaced with FFT on the steering vectors of conventional frequency-domain beamforming. The FFT computation method increases the computation speed by hundreds of times compared to SHSEM [17], however this method still needs be applied for several times when dealing with broadband sound source, which increases its computation time.

This paper proposed a new approach, which combines the FFT computation method and the expressions of time-domain methods. This new approach has high computational efficiency for multiple considered frequencies. The detail of this approach is introduced in Sec. 2. The results from this approach are compared to those from SV-C2 [5] and the ray casting method [15] by a simulation benchmark case and an axial fan experiment in Sec. 3. Conclusions are given in Sec. 4.

2 Methods

2.1 Virtual rotating array beamforming

Fig. 1 shows a sketch of rotating sound source localization measurement. The sound source rotates at an angular speed of Ω , which is positive when the rotation is counter-clockwise looking from the microphone array. The microphone array is located at plane $z = 0$ and contains M microphones. The scanning plane is located at plane $z = Z_0$ and contains S grids. The coordinate origin is placed on the rotation axis of sound source. φ is the azimuthal angle from the positive x axis , and θ is the elevation angle from the positive z axis. The position vector of the stationary microphones is $\mathbf{X}$=[$\mathbf{x}_1$, ..., $\mathbf{x}_m$, ..., $\mathbf{x}_M$]$^{\mathrm{T}}$, with $\mathbf{x}_m$=(r_m, φ_m, θ_m), where $(\cdot)^{\mathrm{T}}$ denotes the non-conjugate transpose. The position vector of the scanning plane grids is $\mathbf{Y}$=[$\mathbf{y}_1$, ..., $\mathbf{y}_s$, ..., $\mathbf{y}_S$]$^{\mathrm{T}}$, with $\mathbf{y}_s$=(r_s, φ_s, θ_s).

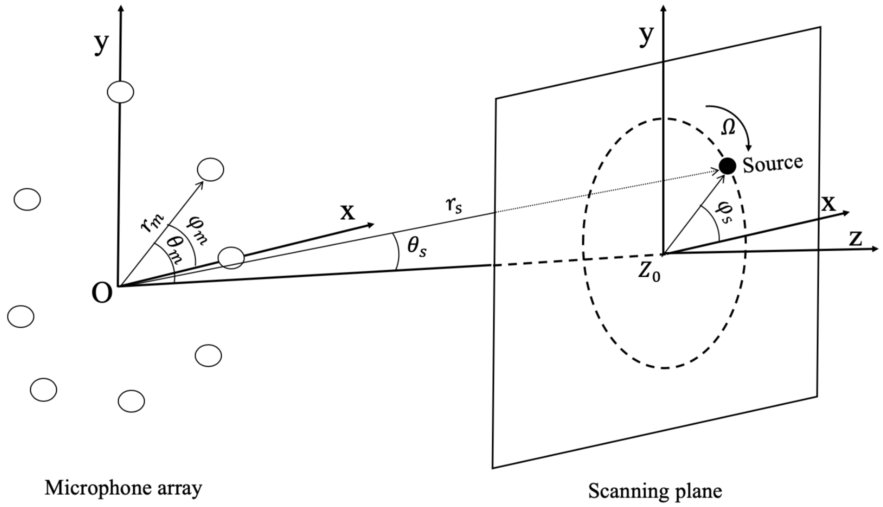

Figure 1: Sketch of phased microphone array measurement for rotating source localization.

The VRA beamforming at angular frequency ω at $\mathbf{y}_s$ is expressed as

$$B(\mathbf{y}_s,\omega) = \mathbf{h}_\Omega^{\mathrm{H}}(\mathbf{y}_s,\omega)\mathbf{C}_\Omega(\omega)\mathbf{h}_\Omega(\mathbf{y}_s,\omega) \tag{1}$$

where $(\cdot)^{\mathrm{H}}$ denotes the conjugate transpose, $(\cdot)_\Omega$ denotes parameter in the rotating frame. $\mathbf{C}_\Omega(\omega)$ and $\mathbf{h}_\Omega(s,\omega)$ are cross-spectral matrix (CSM) and normalized steering vector (SV), respectively.

The CSM is defined as:

$$\mathbf{C}_\Omega(\omega) = \varepsilon\left[\mathbf{p}_\Omega(\omega)\mathbf{p}_\Omega^{\mathrm{H}}(\omega)\right] \tag{2}$$

where $\varepsilon(\cdot)$ denotes the expectation, and

$$\mathbf{p}_\Omega = [p_\Omega(\mathbf{x}_1,\omega),\ldots,p_\Omega(\mathbf{x}_m,\omega),\ldots,p_\Omega(\mathbf{x}_M,\omega)]^{\mathrm{T}} \tag{3}$$

where $p_\Omega(\mathbf{x}_m,\omega)$ is the complex sound pressure spectrum at ω at the mth virtual rotating microphone. The time-domain sound pressure signals at virtual microphones are interpolated from the pressures at real stationary microphones [3–5].

The normalized SV

$$\mathbf{h}_\Omega(\mathbf{y}_s,\omega) = \text{Normalized}([g_{\text{vra}}(\mathbf{x}_1,\mathbf{y}_s,\Omega,\omega),\ldots,g_{\text{vra}}(\mathbf{x}_m,\mathbf{y}_s,\Omega,\omega),\ldots,g_{\text{vra}}(\mathbf{x}_M,\mathbf{y}_s,\Omega,\omega)]^{\mathrm{T}}) \tag{4}$$

where Normalized$(\cdot)$ denotes the normalization formulation. There are several normalized steering vector formulations in the literature and the formulation III in Ref. [13] is used in this paper. $g_{\text{vra}}(\mathbf{x}_m,\mathbf{y}_s,\Omega,\omega)$ is the steering vector propagating from the sth grid point to the mth virtual rotating microphone.

Expressions of $g_{\text{vra}}(\mathbf{x}_m,\mathbf{y}_s,\Omega,\omega)$ will be introduced in Sec. 2.2.

2.2 Modal expansion expression and time-domain expression of steering vector in VRA beamforming

For $g_{\mathrm{vra}}(\mathbf{x}_m, \mathbf{y}_s, \Omega, \omega)$, there are two main expression in the literature [5–8, 10, 12], the modal expansion expression and the time-domain expression. $g_{\mathrm{vra}}(\mathbf{x}_m, \mathbf{y}_s, \Omega, \omega)$ computed through the two expressions have been checked to be equal [5, 12].

The modal expansion expression [6–8, 10] of $g_{\mathrm{vra}}(\mathbf{x}_m, \mathbf{y}_s, \Omega, \omega)$ is

$$g_{\mathrm{vra}}(\mathbf{x}_m, \mathbf{y}_s, \Omega, \omega) = \sum_{m_0=-\infty}^{+\infty} G(\mathbf{x}_m, \mathbf{y}_s, m_0, \omega + m_0\Omega) \tag{5}$$

where $G(\mathbf{x}_m, \mathbf{y}_s, m_0, \omega + m_0\Omega)$ is the modal transfer function of sound field generated by rotating sources. In SHSEM, $G(\mathbf{x}_m, \mathbf{y}_s, m_0, \omega + m_0\Omega)$ is expressed as a spherical harmonic series expansion [8, 10]. In the FFT computation method, $G(\mathbf{x}_m, \mathbf{y}_s, m_0, \omega + m_0\Omega)$ is expressed as a discrete Fourier transformation on the steering vectors of conventional frequency-domain beamforming [17].

The time-domain expression [5, 12] of $g_{\mathrm{vra}}(\mathbf{x}_m, \mathbf{y}_s, \Omega, \omega)$ is

$$g_{\mathrm{vra}}(\mathbf{x}_m, \mathbf{y}_s, \Omega, \omega) = \frac{\mathrm{e}^{-\mathrm{i}\omega\tau_{sm}}}{4\pi r_{\mathrm{decay}}} \tag{6}$$

where τ_{sm} is the sound travel time from the sth grid point to the mth virtual rotating microphone, r_{decay} is the scaled sound travel distance,

$$r_{\mathrm{decay}} = c_0\tau_{sm}(1 - |\Omega r_m/c_0|\cos(\varphi_{sm})) \tag{7}$$

and φ_{sm} is the angle between the distance vector from the sth grid point to the mth virtual rotating microphone and the reverse velocity vector of the mth virtual rotating microphone [5]. In SV-C2, τ_{sm} is calculated by numerically solving a transcendental equation [5, 12]. In ray casting method, τ_{sm} is estimated by numerically solving a system of ordinary differential equations (ODE) [15]. τ_{sm} and r_{decay} are independent of ω and only needs to be calculated once when dealing with multiple frequencies.

A new approach, which combines the FFT computation method and the time-domain expression, will be introduced in Secs. 2.3 and 2.4.

2.3 FFT computation method of the VRA steering vector at a single frequency

According to the research by Zhang & Ma [17], $G(\mathbf{x}_m, \mathbf{y}_s, m_0, \omega + m_0\Omega)$ can be approximated as a discrete Fourier transformation on the steering vectors of conventional frequency-domain beamforming,

$$G(\mathbf{x}_m, \mathbf{y}_s, m_0, \omega + m_0\Omega) = \frac{1}{M_0} \sum_{m_2=1}^{M_0} \frac{\mathrm{e}^{-\mathrm{i}\frac{(\omega+m_0\Omega)}{c_0} r_{sm}(\phi_{m_2}+\varphi_m-\varphi_s)}}{4\pi r_{sm}(\phi_{m_2} + \varphi_m - \varphi_s)} \mathrm{e}^{-\mathrm{i}m_0\phi_{m_2}} \tag{8}$$

where $r_{sm}(\phi_{m_2} + \varphi_m - \varphi_s)$ is the distance between $(r_m,\ \phi_{m_2} + \varphi_m,\ \theta_m)$ and $(r_s,\ \varphi_s,\ \theta_s)$, and $\phi_{m_2} = 2\pi(m_2 - 1)/M_0$. M_0 is the maximum summation index and its value will be discussed in

Sec. 3.3. FFT is used to compute the right-hand side of Eq. (8). Then $G(\mathbf{x}_m, \mathbf{y}_s, m_0, \omega + m_0\Omega)$ is substituted into the following equation to calculate $g_{\mathrm{vra}}(\mathbf{x}_m, \mathbf{y}_s, \Omega, \omega)$.

$$g_{\mathrm{vra}}(\mathbf{x}_m, \mathbf{y}_s, \Omega, \omega) = \sum_{m_0=-M_0/2}^{M_0/2-1} G(\mathbf{x}_m, \mathbf{y}_s, m_0, \omega + m_0\Omega) \tag{9}$$

Detailed steps are as follows. Firstly a $1 \times M_0$ vector $\mathbf{V}(\mathbf{x}_m, \mathbf{y}_s, \omega + m_0\Omega)$ is constructed,

$$\begin{aligned}\mathbf{V}(\mathbf{x}_m, \mathbf{y}_s, \omega + m_0\Omega) = [&\frac{\mathrm{e}^{-\mathrm{i}\frac{(\omega+m_0\Omega)}{c_0} r_{sm}(0+\varphi_m-\varphi_s)}}{4\pi r_{sm}(0+\varphi_m-\varphi_s)}, \cdots, \frac{\mathrm{e}^{-\mathrm{i}\frac{(\omega+m_0\Omega)}{c_0} r_{sm}(2\pi\frac{(m_2-1)}{M_0}+\varphi_m-\varphi_s)}}{4\pi r_{sm}(\frac{2\pi(m_2-1)}{M_0}+\varphi_m-\varphi_s)}, \cdots, \\ &\frac{\mathrm{e}^{-\mathrm{i}\frac{(\omega+m_0\Omega)}{c_0} r_{sm}(\frac{2\pi(M_0-1)}{M_0}+\varphi_m-\varphi_s)}}{4\pi r_{sm}(\frac{2\pi(M_0-1)}{M_0}+\varphi_m-\varphi_s)}]\end{aligned} \tag{10}$$

Through FFT,

$$\mathbf{V}_{\text{fft, shifted}}(\mathbf{x}_m, \mathbf{y}_s, \omega + m_0\Omega) = \frac{1}{M_0}\mathscr{F}(\mathbf{V}(\mathbf{x}_m, \mathbf{y}_s, \omega + m_0\Omega)) \tag{11}$$

where $\mathscr{F}$ represents a shifted FFT, which rearranges FFT by shifting the zero-frequency component to the center of the vector. Secondly, a $M_0 \times M_0$ matrix $\mathbf{A}(\mathbf{x}_m, \mathbf{y}_s, \Omega, \omega)$ is constructed by substituting m_0 from $-M_0/2$ to $M_0/2-1$ into $\mathbf{V}_{\text{fft}}(\mathbf{x}_m, \mathbf{y}_s, \omega + m_0\Omega)$ in turn,

$$\begin{aligned}\mathbf{A}(\mathbf{x}_m, \mathbf{y}_s, \Omega, \omega) = [&\mathbf{V}_{\text{fft, shifted}}(\mathbf{x}_m, \mathbf{y}_s, \omega + (-\frac{M_0}{2})\Omega), \\ &\mathbf{V}_{\text{fft, shifted}}(\mathbf{x}_m, \mathbf{y}_s, \omega + (-\frac{M_0}{2}+1)\Omega), \\ &\cdots, \mathbf{V}_{\text{fft, shifted}}(\mathbf{x}_m, \mathbf{y}_s, \omega + (\frac{M_0}{2}-1)\Omega)]^{\mathrm{T}}\end{aligned} \tag{12}$$

Thus $G(\mathbf{x}_m, \mathbf{y}_s, m_0, \omega + m_0\Omega)$ is the $(m_0 + M_0/2 + 1, m_0 + M_0/2 + 1)$th element of matrix $\mathbf{A}(\mathbf{x}_m, \mathbf{y}_s, \Omega, \omega)$. Lastly, according to Eq. (9), $g_{\mathrm{vra}}(\mathbf{x}_m, \mathbf{y}_s, \Omega, \omega)$ equals the sum of the diagonal elements of $\mathbf{A}(\mathbf{x}_m, \mathbf{y}_s, \Omega, \omega)$, i.e.,

$$g_{\mathrm{vra}}(\mathbf{x}_m, \mathbf{y}_s, \Omega, \omega) = \mathrm{trace}(\mathbf{A}(\mathbf{x}_m, \mathbf{y}_s, \Omega, \omega)) \tag{13}$$

This FFT computation method increases the computation speed of $g_{\mathrm{vra}}(\mathbf{x}_m, \mathbf{y}_s, \Omega, \omega)$ by hundreds of times compared to SHSEM, according to Ref. [17]. This method is also faster than time-domain methods at a single frequency.

However this method still has to be applied for several times when dealing with multiple frequencies, which increases its computation time. A technique to dealing with multiple frequencies will be proposed in Sec. 2.4.

2.4 Modified FFT computation method of sound travel time and VRA steering vectors for multiple frequencies

As τ_{sm} and r_{decay} are independent of ω, τ_{sm} and r_{decay} are calculated to deal with multiple frequencies. According to Eq. (6), $(-\omega\tau_{sm})$ is the argument of $g_{\text{vra}}(\mathbf{x}_m, \mathbf{y}_s, \Omega, \omega)$ when $-\pi \leq (-\omega\tau_{sm}) < \pi$, and $\frac{1}{4\pi r_{\text{decay}}}$ is the magnitude of $g_{\text{vra}}(\mathbf{x}_m, \mathbf{y}_s, \Omega, \omega)$. Thus, when choosing a sufficiently low frequency ω' that satisfy $-\pi \leq (-\omega'\tau_{sm}) < \pi$, there are

$$\tau_{sm} = \frac{\text{argument}(g_{\text{vra}}(\mathbf{x}_m, \mathbf{y}_s, \Omega, \omega'))}{-\omega'} \tag{14}$$

$$r_{\text{decay}} = \frac{1}{4\pi\,|g_{\text{vra}}(\mathbf{x}_m, \mathbf{y}_s, \Omega, \omega')|} \tag{15}$$

$\omega' = 1$ rad/s is recommended and the value of ω' will be discussed in Sec. 3.3. Based on Eqs. (13-15), the modified FFT computation method of $g_{\text{vra}}(\mathbf{x}_m, \mathbf{y}_s, \Omega, \omega)$ for multiple frequencies $\omega = \omega_1, \omega_2, ..., \omega_n$ is obtained, including 3 steps.
Step 1: Choose a sufficiently low frequency ω'. Then $g_{\text{vra}}(\mathbf{x}_m, \mathbf{y}_s, \Omega, \omega')$ is computed by substituting $\omega = \omega'$ into Eq. (13).
Step 2: Calculate τ_{sm} and r_{decay} by substituting $g_{\text{vra}}(\mathbf{x}_m, \mathbf{y}_s, \Omega, \omega')$ into Eqs. (14) and (15).
Step 3: Obtain $g_{\text{vra}}(\mathbf{x}_m, \mathbf{y}_s, \Omega, \omega)$ by substituting τ_{sm}, r_{decay} and $\omega = \omega_1, \omega_2, ..., \omega_n$ into Eq. (6).

This modified FFT computation method is denoted as SV-FFT in this paper.

3 APPLICATIONS TO VRA BEAMFORMING

3.1 Simulation: The b11a benchmark case

The b11a benchmark case in Ref. [2] is used to verify SV-FFT in this subsection. Fig. 2 marks the position of the sound source at the trigger instant by a black star and the positions of the 64 microphones by blue dots. For this case, the rotational speed of the sound source is 1500 rpm, the sampling rate is 48 kHz and the scanning plane is divided into 71×71 grids with grid resolution 0.010 m.

Steering vectors of VRA beamforming in the b11a benchmark case are computed via SV-C2 [5], the ray casting method [15] and SV-FFT. The computation is carried out on an Intel Core i5-9300H CPU @2.40GHz with Python 3.7.4 and Acoular 22.3 software package [14]. The computation times for multiple frequencies are counted and shown in Table 1. SV-FFT improves the computational efficiency by an order of magnitude compared with SV-C2 and the ray casting method.

Table 1: Computation times for VRA steering vectors

Number of frequencies	1	10	100
SV-C2, proposed in Ref. [5]	45.8 s	47.1 s	49.1 s
Ray Casting Method, proposed in Ref. [15]	58.9 s	59.1 s	60.2 s
SV-FFT, proposed in this paper	4.7 s	4.8 s	6.1 s

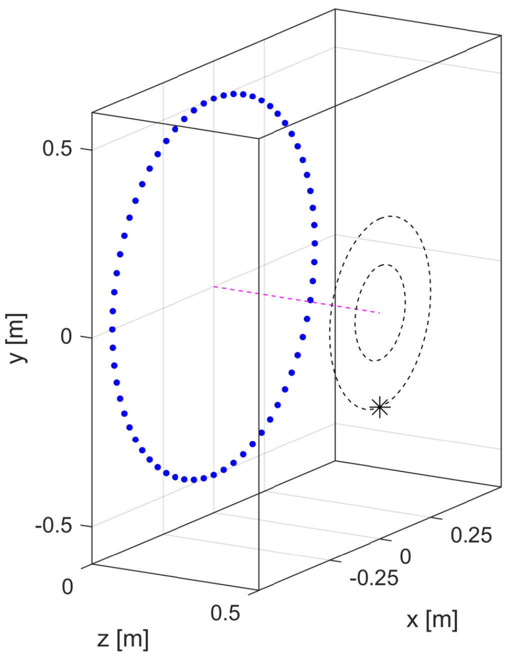

Figure 2: Sketch of the b11a benchmark case. Microphones: blue dots. Source: black star.

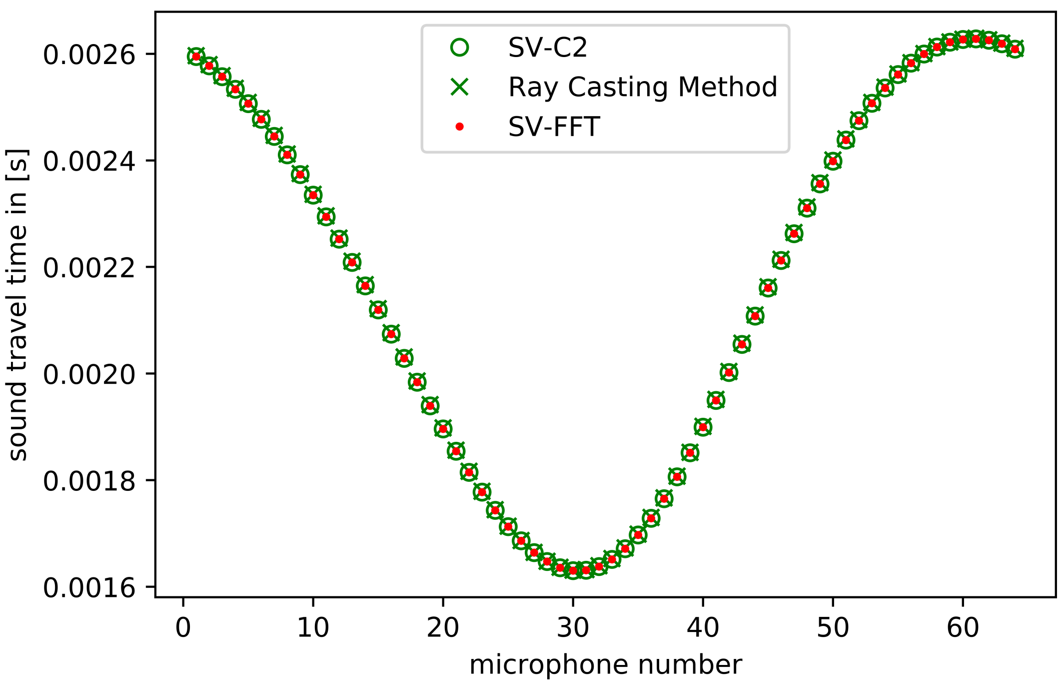

Figure 3: Sound travel time from the rotating source to each of the 64 virtual rotating microphones in the b11a case.

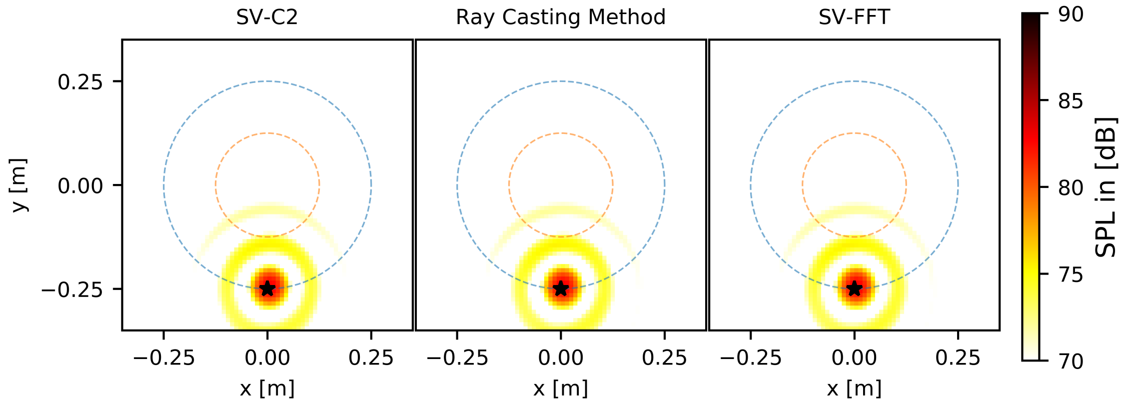

Figure 4: VRA beamforming for third-octave frequency bands at 3 kHz in the b11a case. Sources are marked in black stars.

The computation results show that these three methods are consistent in sound travel time. As an example, the sound travel times from the rotating source to 64 virtual rotating microphones via these three methods are shown in Fig. 3.

As these three methods only differ in the steering vector calculation, the beamforming results are consistent. As an example, VRA beamformings at 3 kHz are shown in Fig. 4.

3.2 Experiment: A five-bladed axial fan

Phased microphone array measurements on a five-bladed axial fan with a rotor diameter of 0.80 m is used in this subsection. Fig. 5 shows the experimental setup. The experiment was conducted in a anechoic chamber. The ring array with 64 microphones and a diameter of 2.09 m is placed 0.74 m in front of the suction side of the fan. The details of setup are introduced in Ref. [15].

SV-FFT, the ray casting method [15] and SV-C2 [5] are used to calculate the sound travel time and the steering vectors. The scanning plane is divided into 97×97 grid points with grid resolution 0.010 m. Inflow field is ignored in the VRA beamforming. The VRA beamforming results in Fig. 6 shows that these methods are similar. This means that the effectiveness of SV-FFT in simulation and experiment application is consistent.

3.3 Discussion

In this subsection, the interrogative sentence at the beginning of each paragraph guides the discussion in that paragraph.

How to choose the value of ω' in the step 1 of SV-FFT? The sound travel time from a grid point to a virtual rotating microphone, i.e. τ_{sm}, is generally less than 1 s for indoor measurements. Thus $\omega' = 1$ rad/s is chosen in this paper, as $-\pi \leq (-\omega' \tau_{sm}) < \pi$ is satisfied. Then $\tau_{sm} = -\text{argument}(g_{\text{vra}}(\mathbf{x}_m, \mathbf{y}_s, \Omega, 1))$.

How to choose the value of maximum summation index M_0 in SV-FFT? Both accuracy and processing time increase when M_0 increases, so M_0 needs to be carefully chosen to balance accuracy and computational efficiency. M_0 should be larger to keep the computational accuracy

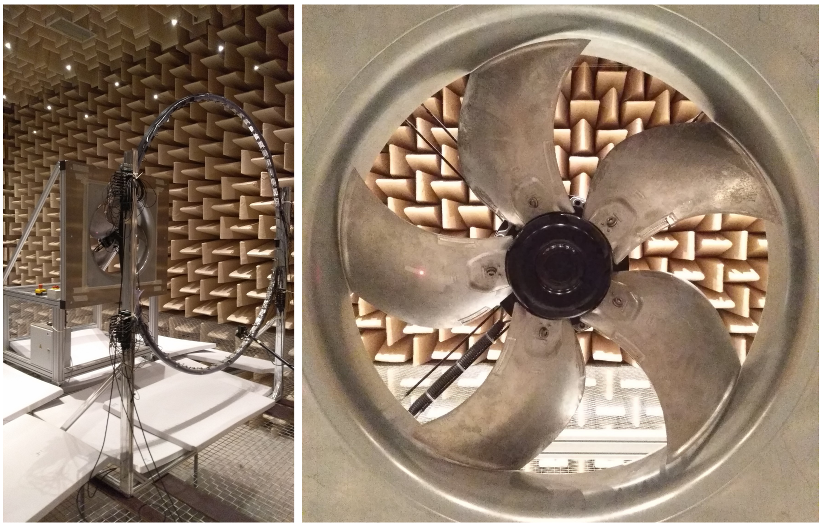

Figure 5: Experimental configuration. Left, experimental setup; right, fan.

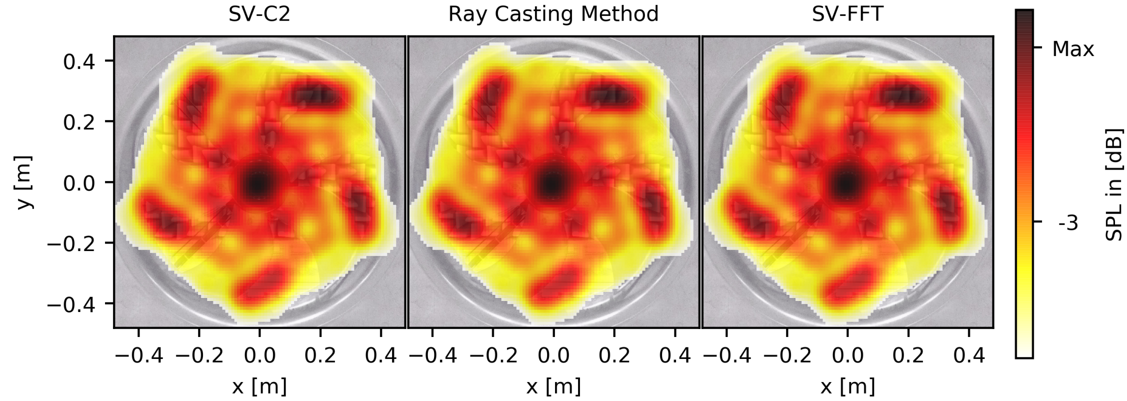

Figure 6: VRA beamforming for third-octave frequency bands at 2 kHz in the five-bladed axial fan experiment.

when ω and Ω increases, and M_0 should be smaller to keep the computational efficiency when ω and Ω decreases. In Ref. [17], $M_0 = 64$ is recommended for subsonic moving broadband sound sources. For SV-FFT in this paper, $M_0 = 16$ is enough since $\omega = \omega'$ is very small. Thus $M_0 = 16$ is used in this paper, and the relative error of sound travel time computation between SV-FFT and SV-C2 is controlled within 0.01% in the simulation case.

Why SV-FFT has a higher computational efficiency? FFT is a fast algorithm, while the computational efficiencies of time-domain methods are limited by the iteration when solving sound travel equations. In addition, SV-FFT is written in vectorized form in Eqs. (10)-(13) , which is suitable for processing by Python.

Is SV-FFT suitable for arbitrary axisymmetric flow? SV-FFT is derived based on the ideal case that the medium is at rest in the stationary reference frame, i.e., medium purely rotates in the virtual rotating frame. So it is not generic and is suitable when no strong refraction occurs in the flow. An improved method which suitable for rotating medium with axial speed and non-constant rotational speed is under research and will be presented in the future.

4 CONCLUSIONS

A modified FFT computation method, denoted as SV-FFT, is proposed in this paper to calculate the sound travel time in rotating medium and the steering vectors in VRA beamforming. Instead of solving sound travel equations or computing spherical harmonic series, this approach is based on the combination of FFT computation method and time-domain expression of VRA steering vector. Firstly, a matrix is constructed by FFT computation on the steering vectors of conventional frequency-domain beamforming at a sufficiently low frequency. Subsequently the sound travel time and the scaled sound travel distance are obtained via computing the argument and magnitude of the trace of the matrix respectively. At last, steering vectors at each considered frequency are calculated efficiently via the sound travel time and the scaled sound travel distance. In the application for b11a benchmark, the accuracy of SV-FFT is verified, and the computational efficiency of SV-FFT improved by an order of magnitude compared with SV-C2 and ray casting method. An experiment for a five bladed fans also validate the effectiveness of SV-FFT.

References

[1] H. Bu, X. Huang, and X. Zhang. "An overview of testing methods for aeroengine fan noise." *Progress in Aerospace Sciences*, 124, 100722, 2021. ISSN 03760421. doi:10.1016/j.paerosci.2021.100722.

[2] G. Herold. "Microphone array benchmark b11: Rotating point sources.", 2017. doi:10.14279/depositonce-8460. URL `http://dx.doi.org/10.14279/depositonce-8460`.

[3] G. Herold and E. Sarradj. "Microphone array method for the characterization of rotating sound sources in axial fans." *Noise Control Engineering Journal*, 63(6), 546–551, 2015. ISSN 0736-2501. doi:Doi10.3397/1/376348.

[4] S. Jekosch and E. Sarradj. "An extension of the virtual rotating array method using arbitrary microphone configurations for the localization of rotating sound sources." *Acoustics*, 2(2), 330–342, 2020. ISSN 2624-599X. doi:10.3390/acoustics2020019.

[5] W. Ma, H. Bao, C. Zhang, and X. Liu. "Beamforming of phased microphone array for rotating sound source localization." *Journal of Sound and Vibration*, 467, 115064, 2020. ISSN 0022460X. doi:10.1016/j.jsv.2019.115064.

[6] W. Ma and C. Zhang. "A frequency-domain beamforming for rotating sound source identification." *The Journal of the Acoustical Society of America*, 148(3), 1602–1613, 2020. ISSN 1520-8524 (Electronic) 0001-4966 (Linking). doi:10.1121/10.0001939.

[7] Y. Mao and C. Xu. "Accelerated method for predicting acoustic far field and acoustic power of rotating source." *AIAA Journal*, 54(2), 603–615, 2016. ISSN 0001-1452 1533-385X. doi:10.2514/1.J054425.

[8] C. Ocker and W. Pannert. "Imaging of broadband noise from rotating sources in uniform axial flow." *AIAA Journal*, 55(4), 1185–1193, 2017. ISSN 0001-1452 1533-385X. doi:10.2514/1.J055309.

[9] C. Ocker and W. Pannert. "Acoustic ray method derived with the concept of analogue gravity for the calculation of the sound field due to rotating sound sources." *Applied Acoustics*, 168, 107422, 2020. doi:10.1016/j.apacoust.2020.107422.

[10] W. Pannert and C. Maier. "Rotating beamforming – motion-compensation in the frequency domain and application of high-resolution beamforming algorithms." *Journal of Sound and Vibration*, 333(7), 1899–1912, 2014. ISSN 0022460X. doi:10.1016/j.jsv.2013.11.031.

[11] M. A. Poletti. "Series expansions of rotating two and three dimensional sound fields." *The Journal of the Acoustical Society of America*, 128(6), 3363–3374, 2010. ISSN 1520-8524 (Electronic) 0001-4966 (Linking). doi:10.1121/1.3506352.

[12] M. A. Poletti and P. D. Teal. "Comparison of methods for calculating the sound field due to a rotating monopole." *The Journal of the Acoustical Society of America*, 129(6), 3513–3520, 2011. ISSN 1520-8524 (Electronic) 0001-4966 (Linking). doi:10.1121/1.3589481.

[13] E. Sarradj. "Three-dimensional acoustic source mapping with different beamforming steering vector formulations." *Advances in Acoustics and Vibration*, 2012, 1–12, 2012. ISSN 1687-6261 1687-627X. doi:10.1155/2012/292695.

[14] E. Sarradj and G. Herold. "A python framework for microphone array data processing." *Applied Acoustics*, 116, 50–58, 2017. ISSN 0003682X. doi:10.1016/j.apacoust.2016.09.015.

[15] E. Sarradj, S. Jekosch, and G. Herold. "An efficient ray tracing approach for beamforming on rotating sources in the presence of flow." In *Proceedings of the 8th Berlin Beamforming Conference, BeBeC-2020-S02*, pages 1–9. 2020.

[16] P. Sijtsma, S. Oerlemans, and H. Holthusen. "Location of rotating sources by phased array measurements." In *7th AIAA/CEAS Aeroacoustics Conference and Exhibit, AIAA 2001-2167*. 2001. doi:10.2514/6.2001-2167.

[17] C. Zhang and W. Ma. "Fast fourier transformation computation of modal transfer function for rotating source localization." *AIAA Journal*, pages 1–5, 2022. doi:10.2514/1.j061179.